JOURNAL

Inhomogeneous Spherical-Earth Finite Element Model of Coseismic Offset due to The 2012 Indian Ocean Earthquake

Cecep Pratama, Takeo Ito, Takao Tabei

Inhomogeneous spherical-earth finite element model of coseismic offset due to the 2012 Indian Ocean Earthquake

Cecep Pratama, Takeo Ito, and Takao Tabei

Citation: AIP Conference Proceedings **1857**, 040002 (2017); doi: 10.1063/1.4987066
View online: http://dx.doi.org/10.1063/1.4987066
View Table of Contents: http://aip.scitation.org/toc/apc/1857/1
Published by the American Institute of Physics

Inhomogeneous Spherical-Earth Finite Element Model of Coseismic Offset due to The 2012 Indian Ocean Earthquake

Cecep Pratama[1, a)] Takeo Ito [1)] and Takao Tabei [2)]

[1]*Graduate School of Environmental Studies, Nagoya University*
D2-2(510), Furo-cho, Chikusa-ku, Nagoya, JAPAN 464-8601
[2]*Department of Applied Science, Faculty of Science, Kochi University*
2-5-1 Akebono-cho, Kochi-shi, Kochi JAPAN 780-8520

[a)] Corresponding author: cecep@seis.nagoya-u.ac.jp

Abstract. On April 11, 2012, a Mw 8.6 earthquake struck off the west coast of northern Sumatra approximately 300 km west of the Sunda trench following by Mw 8.2 two hours afterward. The 2012 Indian Ocean Earthquake sequence, which was the largest intraplate earthquake in recorded history, yielded seismic moment of 1.2-1.3 x 10^{22} N m and 0.2-0.3 x 10^{22} N m for the main shock (Mw 8.6) and the after shock (Mw 8.2), respectively. Aceh GPS Network for Sumatran Fault System (AGNeSS) observed a predominantly ENE coseismic offset up to 10 cm while the sites on the Andaman Island observed southward and southern part Sumatra GPS Array (SuGar) network observed northward. Limited far-field and inland GPS observation network might lead the homogeneous and half-space model insufficient to explain the coseismic offset. In that of sense, in order to estimate more realistic surface displacement due to complex subduction and far-field GPS station, we consider developing inhomogeneous three-dimensional finite element model incorporate subducting slab, three-dimensional velocity earth structure, realistic topography and bathymetry as well as sphericity of the earth. We calculate coseismic offset by forward modeling using slip distribution as reported from Wei et al. [7]. This study investigates the effect of inhomogeneous structure and spherical geometry model in reproducing actual coseimic offset due to 2012 Indian Ocean Earthquake.

INTRODUCTION

The 2012 Indian Ocean Earthquake, which was the largest intraplate earthquake in history of instrumentally recorded event, released a high seismic moment up to 1.6 x 10^{22} N m [4], [7], [9]. Two great earthquakes occurred within two hours observed in an extremely complex conjugate faults, that consist at least three fault planes for Mw 8.6 main shock [4], [7], [9], [10] and one plane for Mw 8.2 aftershock [7]. This great earthquake sequence produced static offsets at GPS station within more than 2000 km distances. This global offsets give us opportunity to observe and analyze the effect of earth structure such as sphericity of the earth and inhomogeneous velocity structure at both near-field and far-field area. In addition, the oceanic intraplate earthquake, which frequently has strike slip faulting, could give us more easy elucidation than the megathrust earthquake due to negligible gravity effect [11], [12].

Existing models, such as Okada [5], compute surface displacement in a half-space earth model assuming homogeneous elastic isotropic and neglect sphericity of the medium. Due to simplify the calculation, slip distribution inversion based on geodetic data widely used these two assumptions. However, current space geodesy and seismological instrument have improved significantly, which has ability to record various natural factors. Moreover, Pollitz [12] and Wang et al. [11] have a set of code to compute in a multilayered and spherical earth medium. Since multilayered or stratified earth medium also classified as inhomogeneous and have been addressed, our target is inhomogeneous structure represented by three-dimensional earth velocity structure.

Several previous studies have been investigated effect of earth rigidity structure [13], [14] and effect of spherical earth [6], [14] in analytical fashion. Here, we utilize offset data from several GPS network around the fault source

International Symposium on Earth Hazard and Disaster Mitigation (ISEDM) 2016
AIP Conf. Proc. 1857, 040002-1–040002-7; doi: 10.1063/1.4987066
Published by AIP Publishing. 978-0-7354-1531-7/$30.00

area (Figure 1). In order to investigate the effect of inhomogeneous earth rigidity structure and sphericity of the earth in numerical framework, we conduct three-dimensional finite element analysis for elastic modeling.

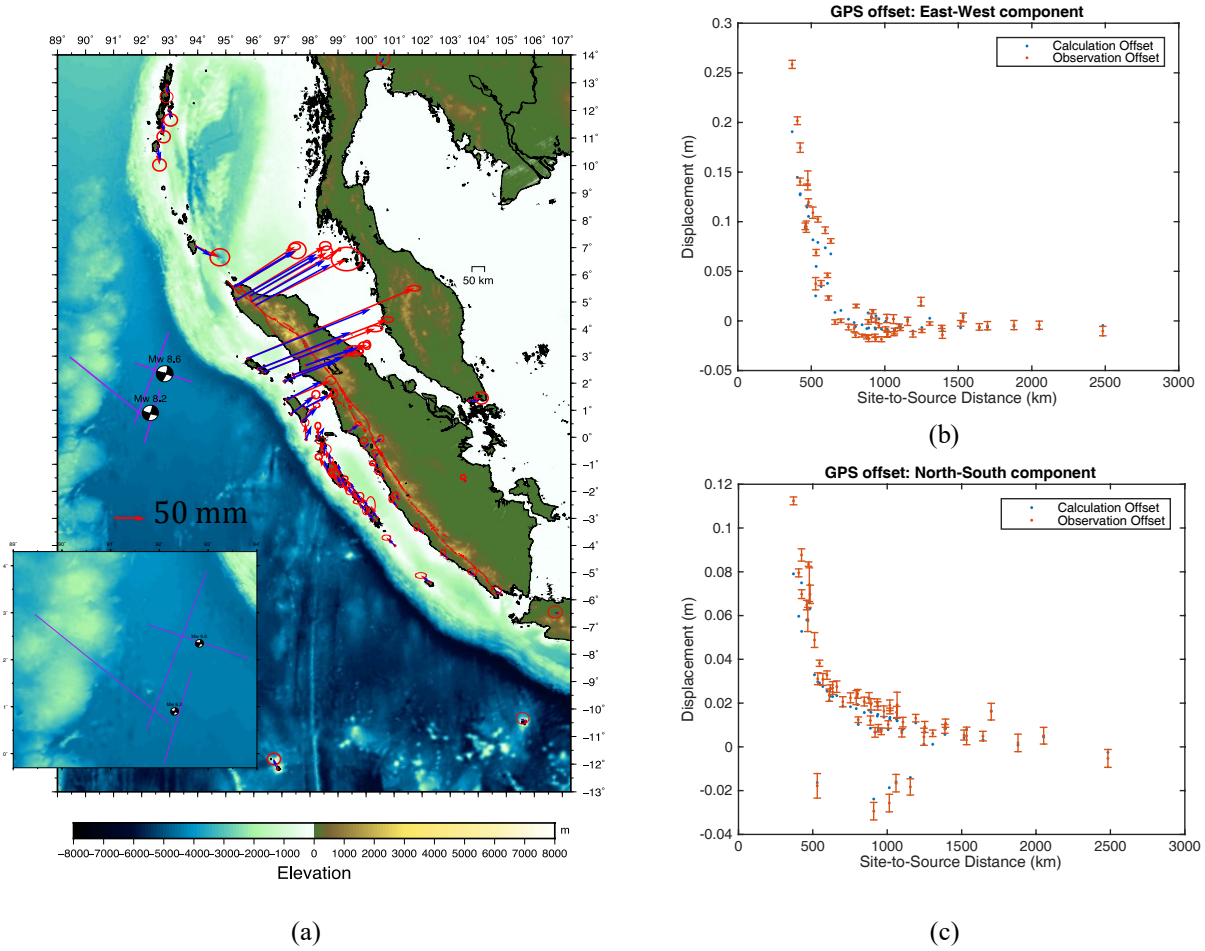

FIGURE 1. Calculation and Observation offset due to the 2012 Indian Ocean Earthquake from AGNeSS, SuGar, IGS and Andaman Island GNSS Networks. (a) Horizontal Component. Red vector as observation offset with 95% standard error circle. Blue vector represent calculation offset, (b) EW offset with red and blue color as (a) caption with 95% standard error bar, (c) NS offset with caption same as (b).

DATA AND METHODS

Observation Data

We analyzed the offset based on daily solution of 4 sites from Aceh GPS Network for the Sumatran fault system (AGNeSS), 1 site from GSI, 6 sites from International GNSS Service (IGS), 5 sites from Andaman and Nicobar island network and 43 sites from Sumatran GPS Array (SuGAr). AGNeSS was developed by Nagoya University, Kochi University, Tohoku University, Institut Teknologi Bandung and Syiah Kuala University, began a couple of month after 2004 Sumatra-Andaman Earthquake [16]. This AGNeSS is very near to the location and has been recorded several earthquake before and after 2012 [15], [16]. Also, postseismic displacement after 2004 Sumatra-Andaman Earthquake was clearly observed by almost both continuous and permanent of AGNeSS [17]. Since AGNeSS located in northern Sumatra, for comparison and assess the other side of Coseismic offset, IGS site and Andaman-Nicobar island site was taken directly from [8] covered far-field and northern side of 2012 Indian Ocean Earthquake source. Meanwhile, SuGAr, along fore-arc, extending from northern to southern region of Sumatra [3], [4].

Receiver Independent Exchange format (RINEX) data for each AGNeSS site was processed using BERNESE 5.0 software [18] with permanent International GNSS Service (IGS) site as a realization in the International Terrestrial Referenee frame 2008 (ITRF 2008) [19]. In this study, we collect total of 118 horizontal and 9 vertical static offset from all available data. AGNeSS recorded very well both horizontal and vertical, while SuGAr has both vertical and horizontal on the northern part of Sumatra near the source location. However, at far-field, SuGAr only have clear horizontal offset.

Coseismic Deformation

The 2012 Indian Ocean Earthquake sequence was nucleate first by the Mw 8.6 mainshock and following by Mw 8.2 aftershock. This largest oceanic intraplate earthquake has a long rupture about 160 s and 60 s for mainshock and aftershock, respectively. It occurred with complex and conjugate fault at diffuse plate boundary [4], [9] with very large amount of slip up to 48 m [4], [10] and deep slip at 60 km depth [7], [20]. Meanwhile from gravity change Han et al. [21] show the dilatation regime along the trench and compressional regime perpendicular to the trench enhance the persistent coseismic deformation with previous studies.

Several finite fault model was proposed to explain the deformation during coseismic. First come from Yue [9] using teleseismic data, and followed by Wei et al [7] and the latest is Hill et al [4] based on high rate GPS and seismic data. Wei et al [7] reported both of mainshock slip distribution and Mw 8.2 aftershock sequence which appropriate with our data that recorded the static displacement in each day. We do not attempt to compare between various coseismic models in this study. Hence, we used coseimic model from Wei et al [7]. We used this finite fault model to do forward modeling in our inhomogeneous spherical earth finite element model.

Finite Element Model

We compiled geometry for creating mesh based on several published model. We adopt surface topography and bathymetry from Becker et al. [22]. Then, for subducted slab along the sunda trench, we derived from seismic tomography result until 300 km [23] and extrapolate down to the 670 km depth. We assumed the slab thickness is 70 km same as the oceanic lithosphere thickness. The size of the model is extending between longitudes 70-115E and latitudes 20S to 20N with 670 km depth. Spherical geometry represented by earth curvature using local geographically referenced Cartesian system that reflects earth-centered earth-fixed (ECEF) coordinate system on the surface as topography and bathymetry that we adopt beforehand (Figure 2). We sweep the surface to the center of the earth and the sweeped geometry was cut by separate slab interface. The mesh consists of more than 5 million tetrahedral element and construct almost 1 million nodal points with the finest element size is 2.5 km near the source area and the subduction region and rough element size at the edge of the model boundary. For simplicity, we set roller condition at each boundary except for the surface. We set free displacement at surface. The finite element mesh is shown in Figure 2.

We conduct finite element method using PyLith code from Computational Infrastructure for Geodynamics with fault interface using domain decomposition method [1]. The PyLith code was widely used for crustal deformation modeling such as elastic modeling [25] or study viscoelastic response [26] and also generates a green's function [27]. It has been benchmarked with the analytic solution such as those in Okada [5]. We use prescribed slip distribution from Wei et al. [7] and simulate the coseismic to produce surface displacement at each site and compare the calculation offset to observation offset.

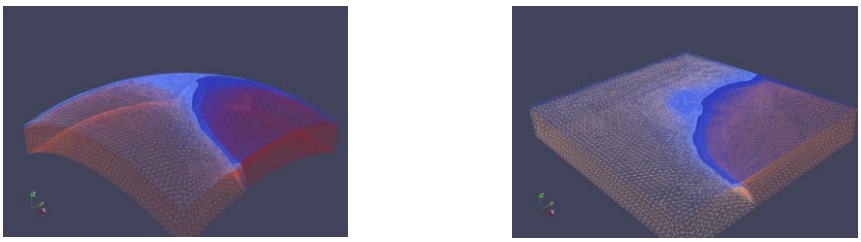

(a) (b)

FIGURE 2. Finite Element Mesh, which has buried fault in the center of the geometry. (a) Spherical-Earth model represent by Earth-Fixed Earth-Centered system, (b) Flat Earth model represent by geographic projection coordinate system.

Inhomogeneous Structure

Since the earthquake is located off western the Sunda trench while the GPS stations are eastern part of the Sunda trench across complex subduction region, the elastic slab have an important factor. Once we incorporate elastic slab, we cannot adopt the multi-layered modulus as widely use in half-space method [5] and spherical-earth method [12]. One possibility that have been done is using uniform rigidity [28], [29] or using inhomogeneous rigidity and density based on 3-D velocity structure. We use 3-D velocity structure following Widiyantoro and Hilst [24] and derived the density using Gardner relationship [31]. We compared with homogeneous value, which are widely used in previous studies [28], [29].

TABLE 1. Inhomogeneous and Homogeneous structures that tested in this study

Parameter	Homogeneous Model	Inhomogeneous Model
Vp	6100 m/s	3-D [24]
Vs	3521.8 m/s	3-D [24]
Density	3300 kg/m^3	3-D
Poisson ratio	0.25	3-D

RESULT AND DISCUSSION

Simulated Offset based on Heterogeneous and Spherical-Earth Model

In this section, we present the calculation based on inhomogeneous and spherical-earth model. In order to evaluate the model, for every GPS site *i*, we evaluate the calculation offset Cal_i and observation offset Obs_i with degree of freedom *df* using reduced Chi-square as following

$$\chi^2 = \frac{1}{df}\sum_{i=1}^{N}\left(\frac{Obs_i - Cal_i}{\sigma_i}\right)$$

Inhomogeneous and spherical-earth model coseismic offset shows smaller values than observation offset (Figure 1). The Figure 1b and Figure 1c also shows that between calculation offset and observation offset has large discrepancy below 500 km site-to-source distances. The offset below 500 km might be affected also by slip model. Since we did not analyze other coseismic model, we could not discuss this possibility. The calculation model has reasonable offset due to our coseismic slip from We et al. [7] that neglect three-dimensional heterogeneous and spherical structures. In that of sense, the effects of inhomogeneous and spherical structures reduce the calculation-offset values. Hence, slip amount will have to be larger than the current model-predicted when the model incorporate heterogeneous structures. For further study such as postseismic deformation analysis, we should scale up the slip amount to obtain appropriate stress and realistic offset. To obtain the big-pictures of misfit offset, we calculate the total misfit using different model as described on the Table 2.

Earth Model Effect Comparison

Inhomogeneous versus Homogeneous

In order to obtain exact value of inhomogeneous and spherical effect, we calculate each model and compare the result. In the following figure, instead of separate EW and NS component offset, the values of displacements are combination from EW and NS component offset. For simplicity, we evaluate the effect using linear relationship. The effect of inhomogeneous structure compared with homogeneous structure, which has density 3300 kg/m^3 and poisson ratio 0.25, produce 30% difference at near field and increase to be 35% at far field. This result agrees with previous studies that the effect of multilayered earth structures gives significant effect to elastic deformation in analytical form [11], [12], [14]. It is comparable since we use 3-D earth velocity structures derived from 1-D multilayered earth structures [24]. The difference around fault region (distance < 100 km) about 25% is due to difference poisson ratio between inhomogeneous structure and homogeneous structure. Thus, the effect of variability

of rigidity gives 5-10% difference. Figure 3 shows that offset value of homogeneous structure is larger than inhomogeneous structure. Hence, the inhomogeneous structure reduces the coseismic offset.

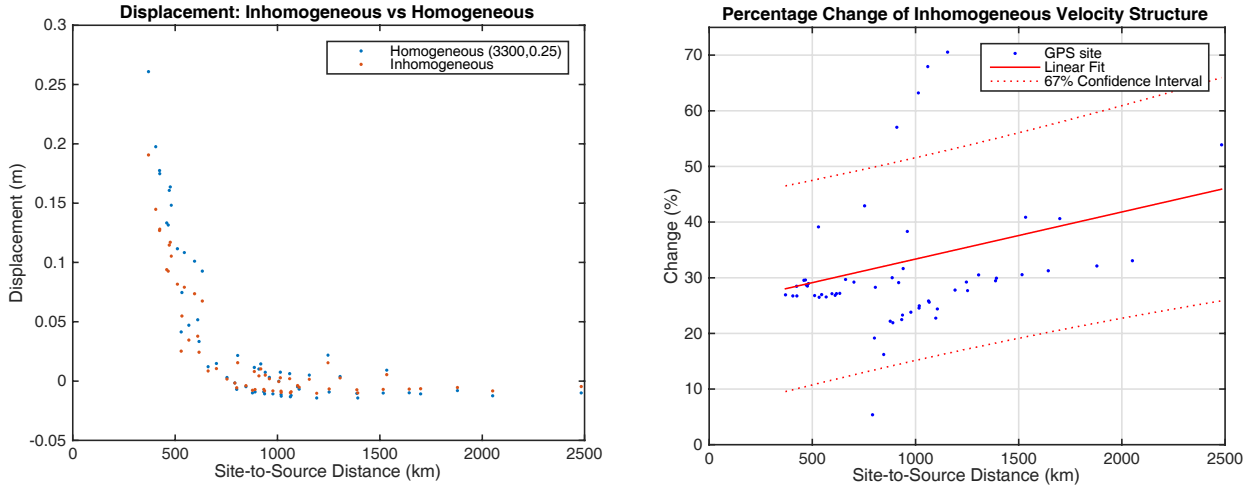

(a) (b)

FIGURE 3. Near-field and far-field GPS static offsets comparison due to Inhomogeneous structure effect. (a) Horizontal GPS component offset, (b) Percentage change between inhomogeneous and homogeneous structure.

Spherical Earth versus Flat Earth

As inhomogeneous structure case, we fixed other earth structures and change the spherical earth and flat earth to obtain the difference. In this case, we changed the mesh between spherical mesh to flat mesh (Figure 2b). We cannot discuss the effect below 400 km and above 2000 km due to dataset limitation. However, using linear fitting, the effect start arise from 100 km site-to-source distance. Spherical earth effect produces 5% difference at near field and 25% at far field. The result also consistent with previous studies [6], [14] that was done within 300 km site-to-source distance in analytic ways. Figure 4 shows that offset value at near field seems to be larger than far field. However, after we normalized the offset, we obtain the difference at near field is smaller than far field. Hence, the more far GPS point the more significant spherical earth effect.

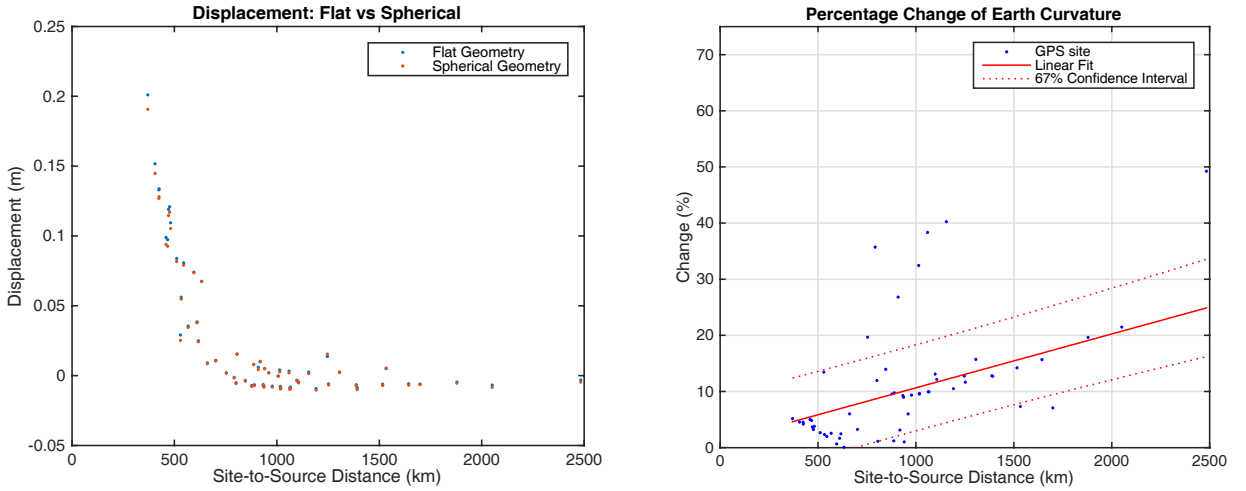

(a) (b)

FIGURE 4. Near-field and far-field GPS static offsets comparison due to spherical shape effect. (a) Displacement for flat geometry and spherical geometry. (b) Percentage change of earth curvature effect as represented by spherical geometry.

TABLE 2. Evaluation of each model compared to observation data

Model Configuration	χ^2		
	EW	NS	Total
Inhomogeneous + Spherical Model	37.25	18.01	55.26
Inhomogeneous + Flat Model	28.41	11.34	39.75
Homogeneous + Spherical Model	33.36	7.61	40.97

CONCLUSION

We have been addressed the effect of inhomogeneous rigidity structure and spherical earth model based on coseismic offset due to 2012 Indian Ocean Earthquake. Despite of limitation of our dataset below 400 km site-to-source distance, based on our result we conclude that

- Inhomogeneous and spherical earth structures are indispensable factor to improved elastic modeling based on far-field offsets. For more than 400 km site-to-source distance, the effect of inhomogeneous rigidity and spherical earth structures are 5-10% and 5-25%, respectively.
- Consideration for inversion analysis to include inhomogeneous and spherical earth structures on elastic Greens Function.
- Our result suggest to scale up slip amount if we use Wei et al. [7] model as a fault model in postseismic deformation analysis.
- For further research, we consider to continue our analysis to investigate comprehensive structures including topography and bathymetry effect, and subducted elastic slab on elastic and viscoelastic modeling.

ACKNOWLEDGMENTS

The author would like to thank CIG Geodynamics for providing FEM Code. This study was partially supported by Monbukagakusho Scholarship from the Ministry of Education, Sports, Science, and Technology of Japan. The map figure is generated by the Generic Mapping Tools [30].

REFERENCES

1. B.T. Aagaard, M.G. Knepley and C.A. Williams, *A domain decomposition approach to implementing fault slip in finite element models of quasi-static and dynamic crustal deformation,* Journal of Geophysical Research: Solid Earth, 118 (2013)
2. B.T. Aagaard, S. Kientz, M.G. Knepley, L. Strand, and C.A. Williams, *Pylith User Manual: version 2.1.0*, Davis, California: Computational Infrastructure of Geodynamics (2013)
3. L. Feng, E.M. Hill, P. Banerjee, I. Hermawan, L.L.H. Tsang, D.H. Natawidjaja, B.W. Suwargadi, and K. Sieh, *A Unified GPS-based earthquake catalog for the Sumatran plate boundary between 2002 and 2013,* Journal Geophysical Research: Solid Earth, 120, 3566-3598 (2015)
4. E.M. Hill, H. Yue, S. Barbot, T.Lay, P.Tapponnier, I. Hermawan, J. Hubbard, P. Banerjee, L. Feng, D.H. Natawidjaya, and K. Sieh, *The 2012 Mw 8.6 Wharton Basin sequence: A cascade of great earthquakes generated by near-orthogonal, young, oceanic mantle faults,* Journal of Geophysical Research: Solid Earth, 120, 3723-3747 (2015)
5. Y. Okada, *Internal deformation due to shear and tensile faults in a half-space,* Bull. Seismol. Soc. Am., 82, 1018-1040 (1992)
6. C. Nostro, A. Piersanti, A. Antonioli, and G. Spada, *Spherical versus flat models of coseismic and postseismic deformations,* Journal of Geophysical Research, 104(B6), 13115-13134 (1999)
7. S. Wei, D. Helmberger, and J.-P. Avouac, *Modeling the 2012 Wharton Basin earthquakes off-Sumatra: Complete lithospheric failure,* Journal Geophysical Research: Solid Earth, 118, 3592-3609 (2013)
8. R.K. Yadav, B. Kundu, K. Gahalaut, J. Catherine, V.K. Gahalaut, A. Ambikapthy, and M.S. Naidu, *Coseismic offsets due to the 11 April 2012 Indian Ocean Earthquakes (Mw 8.6 and 8.2) derived from GPS measurements,* Geophysical Research Letters, 40, 3389-3393 (2013)

9. H. Yue, T. Lay, and K.D. Koper, *En echelon and orthogonall fault ruptures of the 11 April 2012 great intraplate earthquakes,* Nature, 490, 245-249 (2012)
10. C. Satriano, E. Kiraly, P. Bernard, and J.-P Vilotte, *The 2012 Mw 8.6 Sumatra earthquake: Evidence of westward sequential seismic ruptures associated to the reactivation of a N-S ocean fabric,* Geophys. Res. Lett., 39, L15302 (2012)
11. R. Wang, F.L. Martin, and F. Roth, *PSGRN/PSCMP-a new code for calculating co- and post-seismic deformation, geiod and gravity changes based on the viscoelastic-gravitational dislocation theory,* Comput. Geosci., 32, 527-541 (2006)
12. F.F. Pollitz, *Gravitational viscoelastic posteseismic relaxation on a layered spherical earth,* Journal Geophysical Research, 102(B8), 17921-17941 (1997)
13. P. Banerjee, F. Pollitz, and R. Burgmann, *Size and duration of the great 2004 Sumatra-Andaman earthquake from far-field static offsets,* Science, 308, 1769-1772 (2005)
14. J. Dong, W. Sun, X. Zhou, and R. Wang, *Effects of earth's layered structure, gravity and curvature on coseismic deformation,* Geophysical Journal International, 199, 1442-1451 (2014)
15. T. Ito, E. Gunawan, F. Kimata, T. Tabei, I. Meilano, Agustan, Y. Ohta, N. Ismail, I. Nurdin, and D. Sugiyanto, *Co-seismic offsets due to two earthquakes (Mw 6.1) along the Sumatran fault system derived from GNSS measurements,* Earth, Planets and Space, 68:57 (2016)
16. T. Ito, E. Gunawan, F. Kimata, T. Tabei, M. Simons, I. Meilano, Agustan, Y. Ohta, I. Nurdin, and D. Sugiyanto, *Isolating along-strike variations in the depth extent of shallow creep and fault locking on the northern Great Sumatran fault,* Journal of Geophysical Research, 117, B06409 (2012)
17. E. Gunawan, T. Sagiya, T. Ito, F. Kimata, T. Tabei, Y. Ohta, I. Meilano, H.Z. Abidin, Agustan, I. Nurdin, and D. Sugiyanto, *A comprehensive model of postseismic deformation of the 2004 Sumatra-Andaman earthquake deduced from GPS observations in northern Sumatra,* Journal of Asian Earth Sciences, 88, 218-229 (2014)
18. R. Dach, U. Hugentobler, P. Fridez, and M. Meindl, *Bernese GPS Software version 5.0,* Astronomical Institute, University of Bern (2007)
19. Z. Altamimi, X. Collilieux, and L. Metivier, *ITRF2008: an improved solution of the international terrestrial reference frame,* J. Geodesy, 85(8), 457-473 (2011)
20. M. Ishii, E. Kiser, and E.L. Geist, *Mw 8.6 Sumatran earthquake of 11 April 2012: Rare seaward expression of oblique subduction,* Geology, 41(3), 319-322 (2013)
21. S.-C. Han, J. Sauber, and F. Pollitz, *Coseismic compression/dilatation and viscoelastic uplift/subsidence following the 2012 Indian Ocean Earthquakes quantified from satellite gravity observations,* Geophys. Res. Lett., 42 (2015)
22. J.J. Becker, D.T Sandwell, W.H.F Smith, J. Braud, B. Binder, J. Depner, D. Fabre, J. Factor, S. Ingalls, S-H. Kim, R. Ladner, K. Marks, S. Nelson, A. Pharaoh, R. Trimmer, J. Von Rosenberg, G. Wallace, and P. Weatherall, *Global bathymetry and elevation data at 30 arc seconds resolution: SRTM30_PLUS,* Marine Geodesy, 32:4, 355-371 (2009)
23. O. Gudmundson and M. Sambridge, *A regionalized upper mantle (RUM) seismic model,* Journal of Geophysical Research, 103(B4), 7121-7136 (1998)
24. S. Widiyantoro and R.D. Hilst, *Mantle structure beneath Indonesia inferred from high-resolution tomographic imaging,* Geophysical Journal International, 130, 167-182 (1997)
25. T.T. Hines and E.A. Hetland, *Rapid and simultaneous estimation of fault slip and heterogeneous lithospheric viscosity from post-seismic deformation,* Geophysical Journal International, 204, 569-582 (2016)
26. F. Diao, X. Xiong, R. Wang, Y. Zheng, T.R. Walter, H. Weng, and J. Li, *Overlapping post-seismic deformation processes: afterslip and viscoelastic relaxation following the 2011 Mw 9.0 Tohoku (Japan) earthquake,* Geophysical Journal International, 196, 218-229 (2013)
27. Y.-J. Hsu, M. Simons, C. Williams, and E. Casarotti, *Three-dimensional FEM derived elastic Green's functions for the coseismic deformation of the 2005 Mw 8.7 Nias-Simeulue, Sumatra earthquake,* Geochem. Geophys. Geosyst., 12, Q07013 (2011)
28. Y. Hu and K. Wang, *Spherical-Earth finite element model of short-term postseismic deformation following the 2004 Sumatra earthquake,* Journal of Geophysical Research, 117, B05404 (2012)
29. T. Sun, K. Wang, T. Iinuma, R. Hino, J. He, H. Fujimoto, M. Kido, Y. Osada, S. Miura, Y. Ohta, and Y. Hu, *Prevalence of viscoelastic relaxation after the 2011 Tohoku-oki earthquake,* Nature, 514, 84-87 (2014)
30. P. Wessel, W.H.F. Smith, R. Scharroo, J. Luis and F. Wobbe, *Generic Mapping Tools:Improved version released,* Eos Trans. AGU, 94(45), 409 (2013)
31. G.H.F. Gardner, L.W. Gardner, A.R. Gregory, Formation velocity and density – the diagnostic basics for stratigraphic traps: Geophysics, 29, 770-780 (1974)